Journal of Power Sources, 45 (1993) 311–323

Investigation of a novel aqueous aluminum/sulfur battery

Dharmasena Peramunage, Rensl Dillon and Stuart Licht
Department of Chemistry, Clark University, Worcester, MA 01610 (USA)

(Received October 30, 1992; accepted in revised form March 16, 1993)

Abstract

Electrolytic and electrodic effects are investigated for a novel aluminum/sulfur battery based on concentrated polysulfide catholytes and an alkaline aluminum anode. The battery is expressed by aluminum oxidation and aqueous sulfur reduction for an overall battery discharge consisting of:

$$2Al + S_4^{2-} + 2OH^- + 4H_2O \longrightarrow 2Al(OH)_3 + 4HS^- \quad E_{cell} = 1.79V$$

The theoretical specific energy of the Al/S battery (based on potassium salts) is 647 Wh kg^{-1}. A first generation aluminum/sulfur battery is demonstrated with an open-circuit voltage of 1.3 V, and a specific energy of 110 Wh kg^{-1}.

Introduction

There is a growing need for high-capacity, cost-effective batteries for a variety of consumer applications [1]. The light weight, and cost effectiveness of sulfur and polysulfide salts make these attractive cathodic materials for electrochemical energy storage. For example, a variety of metal/molten sulfur batteries have been presented with a primary focus on sodium/sulfur cells. The cells are operated at temperatures of 300 to 350 °C to maintain the sodium, sulfur and the reaction products in a liquid state and to obtain adequate electrolyte conductivity. However, material constraints associated with the requisite high temperatures, corrosion, thermal cycling and cell fabrication are challenges to their development [1].

We previously presented an alternative high faradaic capacity aqueous sulfur redox cell [2]. That cell utilized electrolytes which by mass could accommodate more reducible sulfur than water. The resultant electrolyte retains the high coulombic capacity of molten sulfur battery electrodes [1], yet operates at room temperature and is highly conductive. In a recent letter [3], we introduced a battery which couples the high faradaic capacity of aqueous sulfur with an aluminum anode to exemplify a novel class of Al/S batteries. In this paper, we expand and further this investigation of these new batteries.

Experimental

Analytical grade reagents and distilled, de-ionized water were used throughout. K_2S solutions were prepared as previously described [4]. K_2S_4 is then nominally formed upon addition of sulfur. Anode materials included Alcan International 99.999% Al

0378-7753/93/$6.00

or Alcan International AB50V Al alloy (now available as DH50V) containing >99% Al alloyed with Mg, Sn and Ga. CoS electrodes were formed by electrodeposition of Co at 50 mA/cm^2 from 50 °C 2 M $CoSO_4$, 0.6 M boric acid, 0.2 M NaCl solution onto a 25 μm brass substrate, followed by oxidation in polysulfide solution as previously described [5].

Overpotential measurements were performed with a conventional three-electrode potentiostatic configuration and a Pine AFRDE4X1 potentiostat. Cells were maintained under thermostatic control to ± 0.2 °C. Both miniature (3 cm^2) and larger (60 cm^2) Al/S cells were constructed from sandwiched rectangular 12.5 cm thick lucite blocks separated by flat neoprene spacers. Al/S cells were discharged under constant load conditions with $\pm 1\%$ precision resistors. The efficiency of aluminum utilization was determined by comparing the coulombs generated during cell discharge to the faradaic equivalents available in the consumed mass of the anode. Similarly, the efficiency of hydroxide or polysulfide utilization was determined by comparing the coulombs generated during cell discharge with the faradaic equivalents available in either the anolyte or catholyte.

Theory

In the simplest form the new battery is expressed by aluminum oxidation and sulfur reduction for an overall battery discharge consisting of:

$$2Al + 3S \longrightarrow Al_2S_3 \quad (1)$$

Figure 1 presents a schematic representation of an aluminum/sulfur battery in alkaline aqueous solutions. In alkaline aqueous solutions, the relevant aluminum and polysulfide half-cells are:

$$Al + 3OH^- \longrightarrow Al(OH)_3 + 3e^- \quad -E^0 = -2.30 \text{ V versus SHE} \quad (2)$$

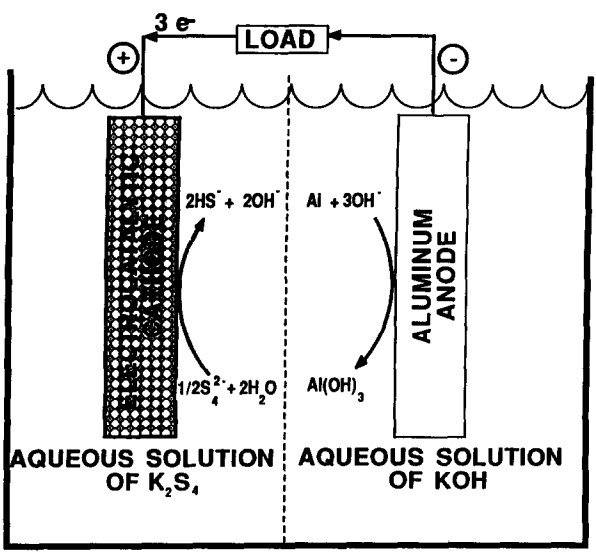

Fig. 1. Schematic representation of an Al/S electrochemical storage cell.

$$S_4^{2-} + 4H_2O + 6e^- \longrightarrow 4HS^- + 4OH^- \quad E^0 = -0.51 \text{ V versus SHE} \tag{3}$$

From eqns. (2) and (3), in alkaline solutions the aluminum/sulfur cell discharge may be summarized as:

$$2Al + S_4^{2-} + 2OH^- + 4H_2O \longrightarrow 2Al(OH)_3 + 4HS^- \quad E_{cell} = 1.79 \text{ V} \tag{4}$$

In accordance with eqn. (4), the faradaic capacity of the Al/S battery (based on potassium salts and all reactants is 361.7 Ah kg^{-1}, and the theoretical specific energy is:

$$1.79 \text{ V} \times 361.7 \text{ Ah kg}^{-1} = 647 \text{ Wh kg}^{-1} \tag{5}$$

This 647 Wh kg^{-1} Al/S specific energy compares favorably with alkaline (Zn/MnO_2), and zinc/silver oxide batteries' theoretical specific energies of 336 and 447 Wh kg^{-1}, respectively. Utilization of lighter weight cations than K^+ may further improve the Al/S energy capacity. The comparable Al/S battery based on sodium salts has respective theoretical current and energy capacities of 522 Ah kg^{-1} and 934 Wh kg^{-1}.

Cathodic couple

In accordance with eqn. (3) the faradaic storage capacity of tetrapolysulfide is:

$$6e^- \text{ per } S_4^- = 6 \text{ faraday (F) per mole } S_4^- = 1254 \text{ Ah kg}^{-1} \; S_4^{2-} \tag{6}$$

The faradaic storage capacity of a polysulfide salt (with the potassium cation) is:

$$6F \text{ per } 206.44 \text{ g } K_2S_4 = 778.9 \text{ Ah kg}^{-1} \; K_2S_4 \tag{7}$$

This theoretical storage capacity of the cathode of 780 to 1250 Ah kg^{-1} (depending on cation) is considerably higher than the theoretical storage capacity of conventional cathodes including 310 Ah kg^{-1} for MnO_2, or 430 Ah kg^{-1} for AgO.

As presented in Fig. 2, K_2s has a substantially higher aqueous solubility than Na_2S. Unlike Na_2S, the high K_2S solubilities parallel those known for sodium and potassium hydroxide solutions. Furthermore, upon addition of sulfur, we determined that up to 33 molal sulfur can be added to 11 molal aqueous K_2S at 50 °C [2]. The resultant electrolyte contains more sulfur than water, and retains the high coulombic capacity of molten sulfur battery electrodes [1], yet operates at room temperature and is highly conductive. In accordance with eqns. (2) and (4), at 25 °C, the solubility of K_2S_4 is consistent with 500 Ah kg^{-1} solution, and as demonstrated in the inset of Fig. 2, this may be reduced to the divalent state at faradaic efficiencies approaching 100%.

Aqueous solutions containing sulfur and a sulfide salt, M_xS_y, result in extensive speciation and a complex equilibrium of $M^{(2y/x)+}$, H_2S, HS^-, S^{2-}, S_2^{2-}, S_3^{2-}, S_4^{2-}, S_5^{2-}, H_2O, H^+ and OH^-. The associated equilibria have been investigated and described [6–9]. Reevaluation of the hydrogen sulfide second acid dissociation constant indicates that HS^- and OH^- are the predominant species upon aqueous dissolution of molar level sulfide salts, with insignificant levels of free sulfide, S^{2-} [4]. The 3:1 limit of sulfur to sulfide dissolution in these molar level sulfide solutions reflects the additional significance of tetrasulfide, S_4^{2-}, although the dominant polysulfide chain length can be varied from 2 to 5 upon solution modification [8, 9, 10–12]. The electrochemistry of polysulfide solutions reflects the complex speciation in these solutions, and is affected by solution pH, activity and the ratio of dissolved sulfur per sulfide ($\equiv x$). As seen in the inset of Fig. 2, at a high value of $x = 3$ (the 0% discharged cell), the practical

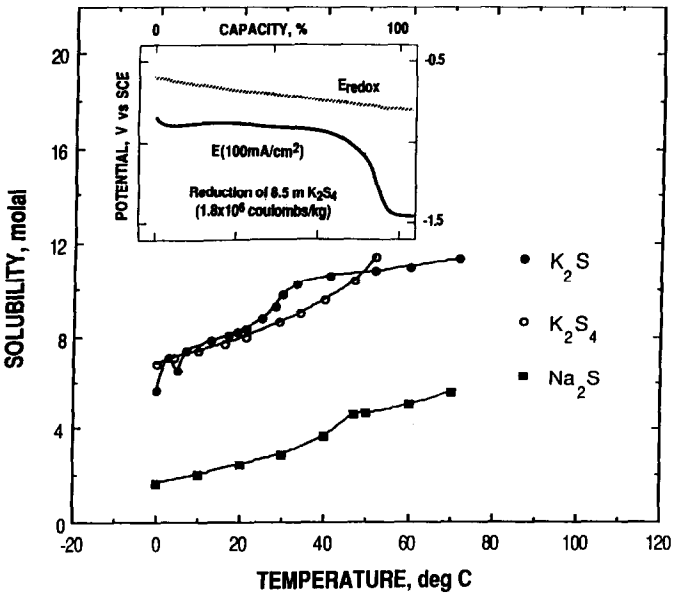

Fig. 2. Aqueous solubility of K_2S_4, Na_2S and K_2S. Inset: reduction of 8.5 M K_2S_4 at 100 mA cm^{-2} on CoS (ref. 2). 100% capacity represents 500 Ah kg^{-1} at 1.79×10^6 C kg^{-1} for 8.5 M K_2S_4 solution in accordance with eqn. (3). Top curve: redox potential, lower curve: discharge potential.

polysulfide redox potential is approximately 100 mV positive (cathodic) compared to eqn. (3), a favorable situation for coupling with an Al anode. The redox potential approaches a value comparable with that of eqn. (3) only in the highly discharged half-cell, and a complete battery is expected to lose 100 mV during discharge due to this variation in the solution-phase redox couple.

Polysulfide solutions are thermodynamically driven to disproportionate to thiosulfate and hydrosulfide. When this process is rapid, the polysulfide solution will degrade via the pentasulfide species [13]:

$$S_5^{2-} + 3OH^- \longrightarrow S_2O_3^{2-} + 3HS^- \tag{8}$$

At a temperature, T(K), the rate of degradation is given by the concentrations of sulfur, hydrosulfide, pentasulfide and the activity of hydroxide [8]:

$$t(\text{days}) = 10^{5600/T-16.6}[S]_{\text{initial}}[HS^-]^2/a_{OH^-}[S_5^{2-}] \tag{9}$$

Our calculations have shown that solution degradation can be minimal in polysulfide solutions without added KOH [8] and at lower (room) temperatures [8, 10–12]. We have calculated that a solution containing 8.47 M K_2S and 12.47 M S has a disproportionation half-life of 3.3 years at 60 °C, but the half-life increases to 164 years at 25 °C [12].

Anodic couple

The faradaic storage capacity of the aluminum anode in accordance with eqn. (2) is given by:

$$3F \text{ per } 26.98 \text{ g Al} = 2981 \text{ Ah kg}^{-1} \text{ Al} \tag{10}$$

As described by eqn. (4), in a complete cell in which one net OH^- is consumed per oxidized Al, the Al faradaic capacity is (assuming potassium salts):

$$3F/(26.98\text{ g Al} + 56.11\text{ g KOH}) = 968\text{ Ah kg}^{-1}\text{ Al} \quad (11)$$

This theoretical storage capacity of the anode of 970 to 3000 Ah kg^{-1} (depending on electrolyte cation, and cathodic half-cell) compares favorably with the maximum theoretical storage capacity of 820 Ag kg^{-1} for Zn.

Al anodes have been investigated for use in aqueous aluminum/silver oxide, aluminum/manganese dioxide, aluminum/air and aluminum/hydrogen peroxide batteries [1]. Effective aluminum anode utilization requires that the rate of electrochemical oxidation, eqn. (2), must be high compared with the parasitic reactions competing with the electrochemical oxidation of Al, which include the reduction of hydrogen and the chemical oxidation of aluminum:

$$H^+ + e^- \longrightarrow 1/2H_2 \quad (12)$$

$$Al + OH^- + 3H_2O \longrightarrow Al(OH)_4^- + 3/2H_2 \quad (13)$$

Spontaneous formation of an aluminum oxide overlayer, and additives introduced either through the solution [14, 15] or by alloying the anode [16, 17] can greatly reduce the parasitic effects of eqns. (12) or (13) as monitored by hydrogen evolution [18]. Observed aluminum oxidation potentials are consistently positive of the thermodynamic potential described by eqn. (2).

Results and discussion

Al/S polarization

Figure 3 represents the measured overpotentials for reduction of a concentrated aqueous polysulfide solution at very thin CoS electrodes. CoS is an effective material to electrocatalyze oxidation and reduction of polysulfide [19]. Over the range of current densities measured, the current–voltage behavior of this solution phase redox couple is approximately linear, and may be summarized by a first order differential of current density with potential. As compiled in this Fig., cathodic polarization losses at thin film CoS electrodes decrease from ~4 to 2 mV cm^2 mA^{-1} as temperature increases from 20 to 65 °C.

Polarization losses for aluminum oxidation have generally not been investigated in highly concentrated (greater than 10 molal) alkaline solutions useful to maximize the specific energy of an Al/S battery. Figure 4 represents the overpotential measured for aluminum oxidation in an 18 M KOH solution. Al oxidation was determined under galvanostatic conditions, and sustained, consistent values are presented without IR compensation. Alternatively, Al oxidation is characterized by hysteresis in potentiostatic sweeps. Small increases in current density were previously observed for Al oxidation in KOH electrolytes with IR correction [20]. Polarization losses decrease from 6 to 0.4 mV cm^2 mA^{-1} as temperature is increased from 20 to 85 °C. Measured polarization is similar in either concentrated sodium or potassium hydroxide electrolytes, and also for aluminum anodes comprised of either 99.999% Al or an Al alloy containing greater than 99% Al and added Mg, Sn and Ga.

To probe cation-selective membrane conductivity, we have discharged Al/S batteries in miniature cells. Each cell membrane studied, Nafion 550 K^+, Raipore R1010 and Raipore HD2291, effectively inhibited polysulfide movement to the anolyte. Miniature

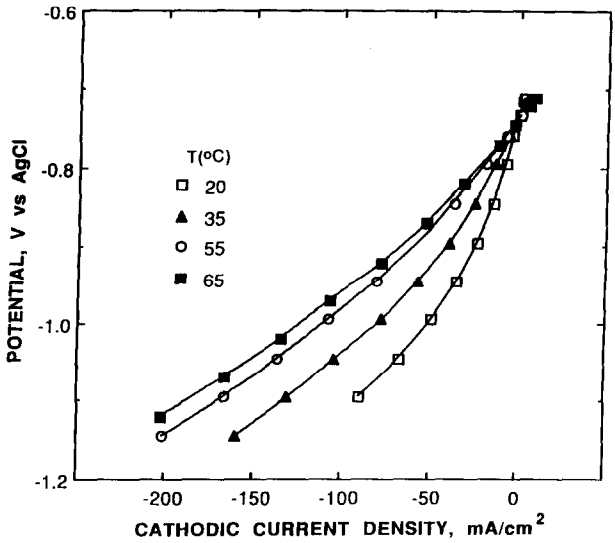

Fig. 3. Potentiostatic reduction of aqueous 7.7 M K_2S_4 on 1 cm^2 CoS on 25 μm brass at a sweep rate of 1 mV s^{-1}.

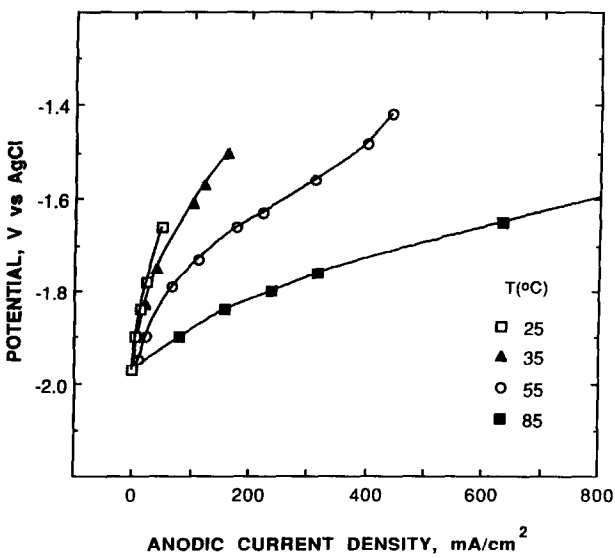

Fig. 4. Oxidation of aluminum (Mg–Sn–Ga aluminum alloy) in stirred aqueous 18 M KOH, 10 mM $In(OH)_3$ at 0.1 mV s^{-1}.

cells were configured in accordance with the schematic of Fig. 1. Each cell contains catholyte and anolyte separated by 3 cm^2 of the membrane under investigation. Cell potential is then measured between a 1.5 cm×2 cm CoS cathode immersed in 0.0005 l 7.7 M K_2S_4 and a 1.5 cm×2 cm Al anode immersed in 0.0005 l aqueous KOH under a variety of applied loads. Of the three, only the sulfonated polyethylene

membrane Raipore HD2291 exhibited the requisite low resistivity flux (10 Ω cm^2) in concentrated (18 M) hydroxide electrolytes. Resistivity of this membrane diminished by a factor of two with temperature increase to 45 °C. Figure 5 compares polarization losses in the miniature cells containing 5.4, 12 and 18 M KOH anolytes. As can be seen in the Fig., polarization losses increase by an order of magnitude with increasing KOH concentration for the Raipore R1010 membrane. At all KOH concentrations tested, polarization losses are smaller with the HD2291 membrane, and do not increase with increasing hydroxide concentration.

Discharge efficiency

In the separated anode/cathode cell configuration represented in Fig. 1, specific energy of the Al/S battery is limited by the mass of alkali hydroxide in the anolyte. To probe efficiency in the Al/S system, we have discharged miniature Al/S batteries with anodic half-cells limited by the available anolytic hydroxide. Cells contain a coulombic excess of both Al and polysulfide. The extent of the parasitic reaction, eqn. (13), is then determined by comparing the coulombs generated during discharge to the faradaic equivalents of solution phase hydroxide in accordance with eqn. (2). At lower concentrations of hydroxide, millimolal concentrations of sodium stannate have been previously found to diminish the rate of hydrogen evolution [14], and improve voltage characteristics of aluminum anodes. As seen in Fig. 6, addition of stannate to highly concentrated (18 M) KOH improves anodic behavior of pure Al. Hence, compared with the stannate free cell, an added 10 mM Na_2SnO_3 in the cell improved the average discharge voltage by 0.1 V, and also improved the utilization of anolytic hydroxide by nearly 10%.

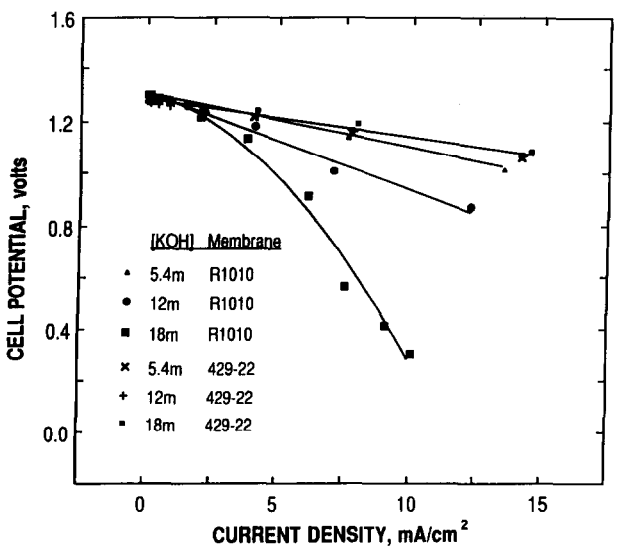

Fig. 5. Membrane effects on polarization of miniature rectangular Al/S cells at 25 °C containing a DHV50V aluminum alloy anode immersed in anolyte and separated by 3 cm^2 of the indicated membrane and a CoS-modified brass cathode immersed in 0.5 ml of 7.7 M K_2S_4 catholyte. Anolyte contains 0.9 ml of the indicated concentration of KOH and 10 mM $In(OH)_3$. Load current is applied by precision resistor.

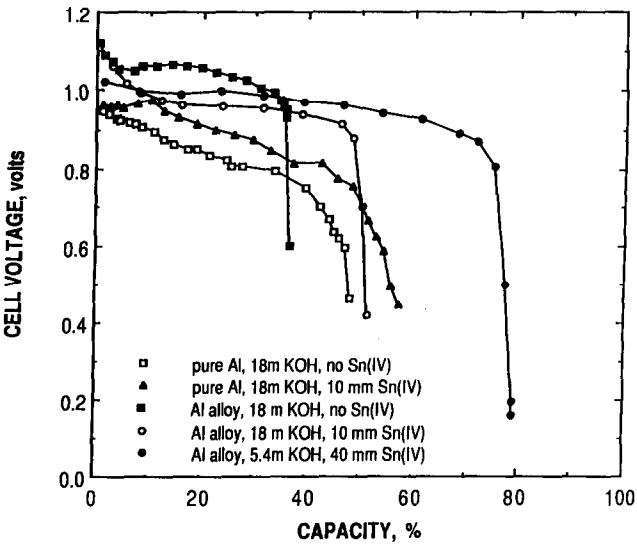

Fig. 6. Effects of adding an anolyte additive, and/or alloying the aluminum anode, on discharge capacity of miniature rectangular Al/S cells at 25 °C. Anodes consist of 99.999% (pure) Al or an alloy containing >99% Al and Mg, Sn and Ga. Cell contains a 1.5 cm×2 cm (both sides exposed) aluminum anode immersed in 0.9 ml 18 M KOH anolyte (w/w 10 mM Na_2SnO_3) and separated on each side by Raipore HD2291 membrane and a 1.5 cm×2 cm CoS-modified brass cathode immersed in 0.5 ml of 7.7 M K_2S_4 catholyte. Cells discharged over a 15 Ω load (~10 mA cm^{-2}). Capacity is determined by comparison of coulombs generated to equivalents of KOH available in the anolyte.

Voltage and efficiency of the anode can also be improved by alloying the aluminum [16, 17]. As seen in Fig. 6, the measured hydroxide coulombic conversion efficiencies in cells containing the stannate-bearing electrolyte and discharged to a potential of 0.7 V, were similar for either a Mg–Sn–Ga aluminum alloy or a 99.999% pure aluminum anode. However, the alloy was characterized by enhanced voltage response and was used in subsequent experiments. In all cases discharge of aluminum was accompanied by generation of a thick white alumina film at the aluminum surface which did not impede cell discharge. Aluminum efficiency was also measured by comparing the coulombs generated during discharge to the mass loss of the washed discharged anode. Trends and magnitudes of aluminum utilization efficiency paralleled those measured for hydroxide utilization efficiency.

At higher discharge current densities, the rate of electrochemical reaction increasingly dominates the competing parasitic chemical reaction, and discharge efficiencies are expected to improve. As seen in Fig. 7, KOH utilization improves from 50 to 60% as current density increases from 10 to 40 mA cm^{-2}. The inset of Fig. 7 compares cell polarization in the charged and 20% discharged cell. Polarization losses improve in the partially-discharged cell, yet open-circuit voltage decreases. These effects tend to offset, and after 20% discharge the cell voltages, compared with those in the charged cell, are improved at current densities greater than 10 mA cm^{-2}. As presented in Fig. 8, amalgamating the 99.999% Al anode by immersion in aqueous mercuric nitrate resulted in coulombic efficiencies approaching 100%. However, as seen in the Fig. inset, this electrode amalgamation also increased polarization losses fourfold to over

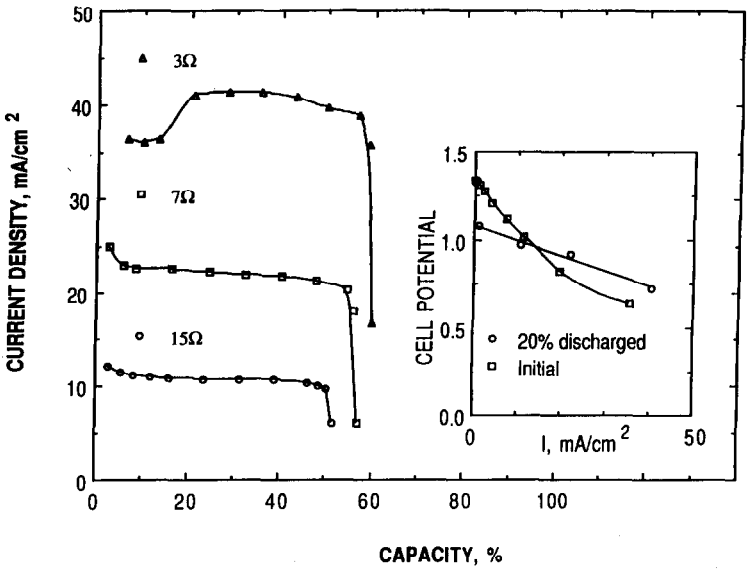

Fig. 7. Effects of current density on voltage and capacity of miniature rectangular Al/S cells at 25 °C. 6 cm^2 Mg–Sn–Ga aluminum alloy anodes employed immersed in 0.9 ml 18 M KOH anolyte and 10 mM Na_2SnO_3. Other cell characteristics are described in the legend of Fig. 6. Inset: Al/S battery cell potential polarization initially and following 20% discharge of the battery.

70 mV cm^2 mA^{-1}. Air exposure of the Hg-modified Al anode resulted in rapid spontaneous oxidation. During discharge, the Hg/Al anode Al/S cell was maintained under argon to prevent this decomposition. In Fig. 8, the 60 h 200 Ω discharge represents a 93% utilization of KOH-limited cell capacity, and the 20 h 35 Ω discharge represents a 72% utilization of available KOH.

Figure 6 includes the enhanced relative utilization of hydroxide at lower (5.4 M) hydroxide concentration in an Al/S battery containing the alloyed Al anode. Alternatively when a 99.999% pure-Al anode was employed, utilization of hydroxide at lower (5.4 M) hydroxide concentration was diminished compared with utilization in a concentrated (18 M) hydroxide anolyte. The Al/S miniature cell tested is limited in specific energy by hydroxide concentration and the challenge remains to increase utilization of hydroxide at high KOH concentrations. To improve KOH conversion utilization, a variety of anolyte additives were studied. Table 1 summarizes the variation of anodic half-cell behavior in Al/S batteries as a series of solution-phase additives are added to an anolyte containing 18 M KOH and 10 mM Na_2SnO_3. Salts such as $Pb(NO_3)_2$ and $K_4P_2O_7$ had no significant effect on discharge capacity. However, several solution–phase additives including KSeCN, dimethyl sulfoxide, $KMnO_4$ K_2SeO_2, and imidazole, markedly improve discharge capacity at additive concentrations of 50 mM or greater. At lower concentrations, several metal oxide salts dramatically effect aluminum anodic behavior.

As seen in Fig. 9, measured Al/S discharge potentials reach a high value with a 10 mM Ga(III) oxide additive. This improvement of over 200 mV is paralleled by a similar improvement in cell open-circuit voltage (to 1.37 V). However, this activated surface is dominated by the parasitic reaction of eqn. (10), as evidenced by rapid hydrogen evolution, excessive heat generation, and <30% utilization efficiencies. Ge(IV),

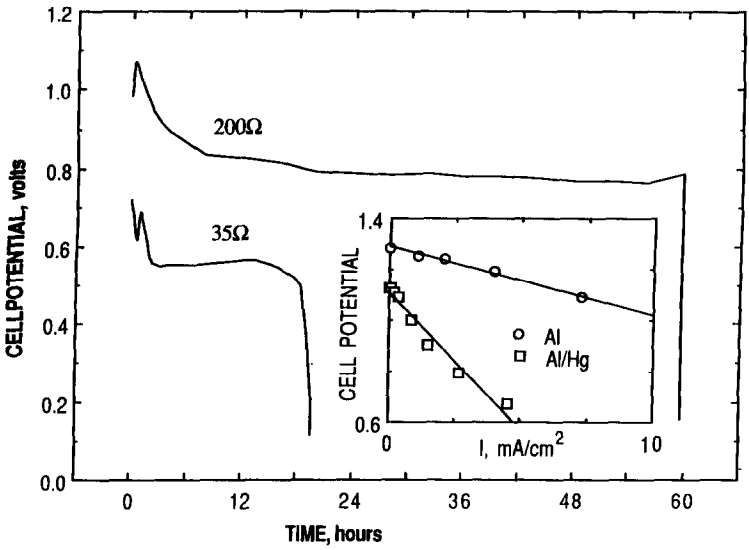

Fig. 8. Effects of aluminum amalgamation on discharge capacity of miniature rectangular Al/S cells at 25 °C. 99.999% Al anodes are pretreated by a 300-s immersion in 1 M HNO_3, 50 mM $Hg(NO_3)_2$ prior to discharge. The resultant glossy Hg overlayer was observed to remain on the surface throughout the anode discharge in 0.9 ml of 18 M KOH and 10 mM Na_2SnO_3. Other cell characteristics are as described in the legend of Fig. 6. Cells discharged at indicated resistive loads at 25 °C. Inset: 25 °C polarization of Al/S cells at various discharge current densities at Al anodes with and without Hg pretreatments.

TABLE 1

Effects of various anolyte additives on 25 °C, 10 mA cm^{-2} discharge of Al/S batteries containing a 1.5×2 cm Mg–Sn–Ga aluminum alloy anode separated on each side by a Raipore HD2291 membrane and CoS-modified brass cathodes immersed in 0.5 ml of 7.7 M K_2S_4 catholyte. Anolyte consists of 0.5 ml 18 M KOH, a 10 mM Na_2SnO_3 additive and the indicated second additive. Capacity is determined by comparison of coulombs generated to 9 mM available KOH in anolyte. Coulombs generated are measured to a discharge voltage of 0.65 V, and median discharge voltages are tabulated

Anolyte additive	Concentration (mM)	V (10 mA cm^{-2})	Capacity (%)
None		0.96	44
$Pb(NO_3)_2$	50	0.93	44
$K_4P_2O_7$	100	0.93	47
KSeCN	250	0.88	56
DMSO	250	0.95	53
$KMnO_4$	25	0.98	56
K_2SeO_2	50	0.88	58
Imidazole	250	0.95	59

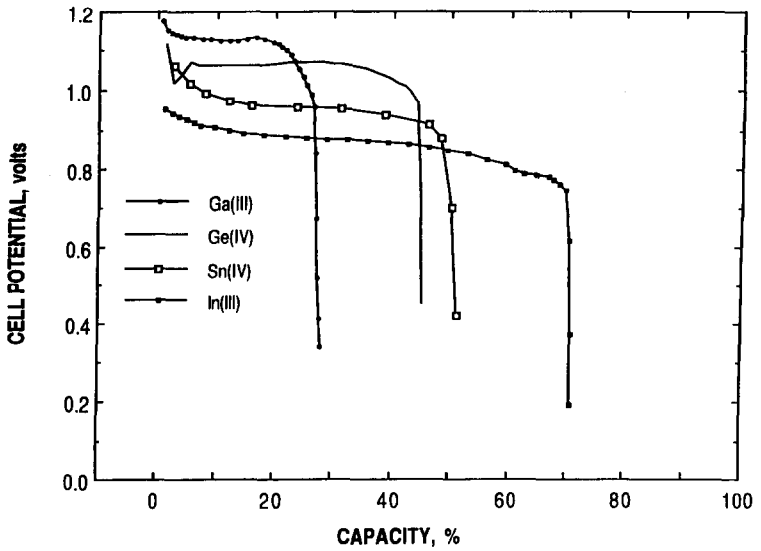

Fig. 9. Effects of various 10 mM metal oxide anolyte additives, on discharge capacity of miniature rectangular Al/S cells at 25 °C. Anolyte contains 18 M KOH, 10 mM of either Ga_2O_3, GeO_2, Na_2SnO_3 or $In(OH)_3$. Other cell characteristics are as described in the legend of Fig. 6.

Sn(IV) and In(II) oxides increase utilization efficiency. Mg(II) or W(VI) (as MgO or Na_2WO_4, not included in Fig. 9) exhibited a capacity and discharge voltage intermediate to the Ga and Sn additives.

The aluminum alloy was particularly stabilized in the $In(OH)_3$ electrolyte. Discharge efficiency, as measured by KOH utilization (shown in Fig. 9) and Al utilization (by anode mass loss, not shown in Fig. 9), increases to greater than 60% with a $In(OH)_3$ additive. Furthermore, the Al usage for the alloy immersed in 0.92 ml 18 M KOH and 10 mM $In(OH)_3$ increased from 67% at 20°C to 80% at 45 °C. The relative volume of anolyte also effects the efficiency of hydroxide utilization. The anodic compartment containing 18 M KOH and 10 mM $In(OH)_3$ was increased in volume from 0.25 to 1.84 ml (increasing theoretical capacity to 0.67 Ah). As shown in Fig. 10, at 35 °C, the increase in anodic capacity is paralleled by an observed increase in KOH utilization from 46 to 79% faradaic conversion efficiencies, and an Al utilization in excess of 80%. In a separate experiment aluminate added to the anolyte decreased utilization efficiency. Hence, this enhancement of faradaic efficiency in the larger volume cells is not related to increased aluminate build-up in the larger volume cell. We hypothesize that increase in faradaic efficiency with anolyte volume may be due to release of Al alloy additives (Mg, Sn and Ga) into the electrolyte during discharge.

Discharge characteristics

Aluminum/sulfur batteries were studied with the sulfonated polyethylene membrane and a volume approximating that of a conventional 'D' cell and containing 60 cm^2 aluminum. Figure 11 presents load and temperature effects on Al/S cells containing 7.7 M K_2S_4 catholyte and 18 M KOH, 10 mM $In(OH)_3$ anolyte. Under these heavy loads, the cells discharge for approximately twice the duration of conventional alkaline (Zn/MnO_2 cells, and up to ten times the duration of zinc/carbon cells [1]. Several Al/S cells were built of similar size (~ 50 ml electrolyte in an initial attempt to optimize

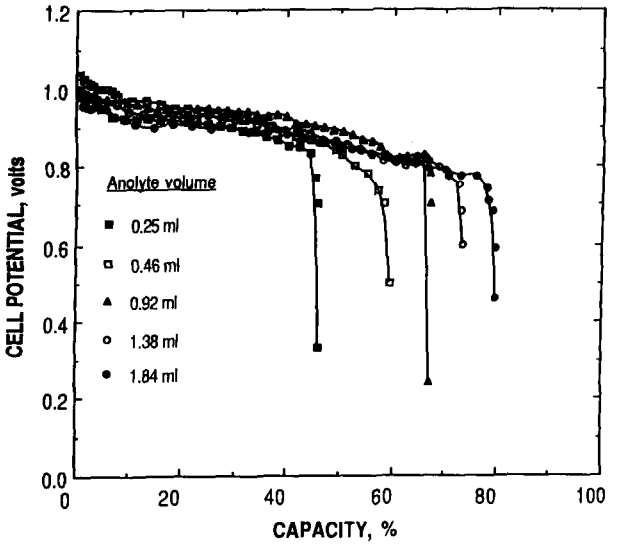

Fig. 10. Effect of anolyte volume on discharge capacity of miniature rectangular Al/S cells at 25 °C. Anolyte contains 18 M KOH and 10 mM $In(OH)_3$. Catholyte contains either 0.52 ml or 1.04 ml of 7.7 M K_2S_4 for cells respectively containing either <1 ml or >1 ml of anolyte. Other cell characteristics are as described in the legend of Fig. 6.

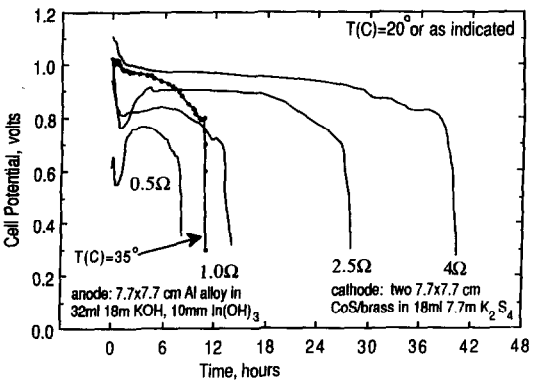

Fig. 11. ~50 ml Al/S cells discharged at various loads for rectangular cells containing 0.018 l 7.7 M K_2S_4 catholyte and 0.032 l 18 M KOH, 10 mM $In(OH)_3$ anolyte and a 60 cm^2 Mg–Sn–Ga aluminum alloy anode separated on each side by 60 cm^2 Raipore HD2291 membrane and a 60 cm^2 thin-film CoS/brass cathode.

specific energy of the battery. These include the discharge at 1.03 Ω for a cell containing 0.030 l 23.3 M (21.1 g H_2O, 27.6 g) KOH, 10 mM (0.05 g) $In(OH)_3$ anolyte and 0.20 l 7.7 M (11.8 g H_2O 18.7 g) K_2S_4 catholyte. The mass of the electrodes (excluding electrical contacts) was 7.4 g for the Al anode, and 4.5 g for the CoS cathode, while the membrane mass was 0.7 g. The cell provided a 13 h, 10.1 Wh discharge. Compared to the mass of cell components, this represents a specific energy of 110 Wh kg^{-1} based on total materials. During discharge, a thick solid $Al(OH)_3$ film develops at the aluminum surface which does not effect cell performance. The 11.4 Ah generated in

the cell represents an 86% conversion efficiency based on KOH, a 78% conversion efficiency based on K_2S_4, and a 68% conversion efficiency based on consumed Al. This first generation specific energy compares favorably with measured specific energies for advanced alkaline (Zn/MnO_2) batteries of 95 Wh kg^{-1} and 130 Wh kg^{-1} for zinc/silver oxide batteries.

Conclusions

This study presents a variety of solution- and solid-phase effects on a novel Al/S battery based on concentrated polysulfide catholytes and an alkaline aluminum anode. The cathodic polysulfide half-cell of the battery displays high storage capacity and a high faradaic conversion efficiency with low polarization losses at CoS thin-film electrocatalytic electrodes. The aluminum half-cell is stabilized in highly concentrated alkaline media by the use of several solution additives including $In(OH)_3$, by alloys of Al, and by increase in anolyte volume.

Several full-cell Al/S battery discharges have been presented. In the complete Al/S cell, open-circuit voltages of up to 1.3 V and a specific energy of 110 Wh kg^{-1} is observed. The theoretical open-circuit voltage of the cell is 1.8 V, and the theoretical specific energy of the Al/S battery (based on potassium salts) is 647 Wh kg^{-1}.

Acknowledgements

The authors are grateful to the Office of Naval Research, The National Science Foundation, the Dreyfus Foundation and the Clark University Carl Julius and Anna (Kranz) Carlson Chair in Chemistry for financial support of this work.

References

1 D. Linden (ed.), *Handbook of Batteries*, McGraw-Hill, New York, 1984.
2 S. Licht, *J. Electrochem. Soc., 134* (1987) 2137; *US Patent No. 4 828 942* (May 9, 1989).
3 S. Licht and D. Peramunage, *J. Electrochem. Soc., 140* (1993) L4.
4 K. Longo, F. Forouzan, D. Peramunage and S. Licht, *J. Electroanal. Chem., 318* (1991) 111.
5 S. Licht and J. Manassen, *J. Electrochem. Soc., 134* (1987) 1064.
6 A. Teder, *Sr. Papperstodn, 72* (1969) 245.
7 W. Giggenbach, *Inorg. Chem., 11* (1972) 1201.
8 S. Licht, J. Manassen, G. Hodes, *Inorg. Chem., 25* (1986) 2486.
9 S. Licht, *Nature, 330* (1987) 148.
10 S. Licht and J. Manassen, *J. Electrochem. Soc., 132* (1985)) 1077.
11 S. Licht, *J. Electrochem. Soc., 133* (1986) 277.
12 S. Licht, G. Hodes and J. Manassen, *J. Electrochem. Soc., 133* (1986) 272.
13 W. Giggenbach, *Inorg. Chem., 13* (1974) 1730.
14 D. D. Mcdonald and C. English, *J. Appl. Electrochem., 20* (1990) 405.
15 W. Bohnstedt, *J. Power Sources, 5* (1980) 245.
16 J. A. Hunter, *US Patent No.* 5 004 654 (Apr. 2, 1991).
17 D. D. Mcdonald, S. Real and M. Urquidi-Mcdonald, *J. Electrochem. Soc., 135* (1988) 2397.
18 S. Real, M. Urquidi-Mcdonald and D. D. Mcdonald, *J. Electrochem. Soc., 135* (1988) 1633.
19 G. Hodes, J. Manassen and D. Cahen, *J. Electrochem. Soc., 127* (1980) 544.
20 D. Chu and R. F. Savinell, *Electrochim. Acta, 36* (1991) 1631.